274 WHOLE ATMOSPHERE DATA ASSIMILATION AND FORECAST EXPERIMENTS

Houjun Wang[1]*, Timothy, J. Fuller-Rowell[1], and Rashid A. Akmaev[2]

[1]CIRES, University of Colorado, Boulder, Colorado
[2]SWPC/NOAA/National Weather Service, Boulder, Colorado

1. INTRODUCTION

Data assimilation is indispensable in any real-world prediction system involving diverse observations. It usually combines a prediction model and data analysis subsystem to make use of the best of both to optimally define a model state. Most often, a model also requires an initialization procedure, such as normal mode initialization, or some sort of digital filters (e.g. Kalnay, 2002) to ensure stability when strongly forced by data. In this study, we explore the extension of the global data assimilation system to the whole atmosphere up to about 600 km altitude.

The period chosen to demonstrate the whole atmospheric data assimilation and forecast system is January-February 2009, during which a very strong sudden stratospheric warming (SSW) occurred. During the SSW Chau et al., (2010) showed that the vertical plasma drift at the magnetic equator over Jicamarca, Peru, changed dramatically, with stronger upward drifts after dawn, reversing to downward drifts in the afternoon. The observations of total electron content (TEC) from ground-based GPS receivers were also shown to change in response to the vertical plasma drift, with a stronger equatorial ionospheric anomaly (EIA) in the morning when the drifts were stronger upward, and with a decrease in TEC when the drifts turned downward. It is speculated that the change in dayside E-region dynamo winds in response to the stratospheric warming are responsible for the change in vertical plasma drift and total electron content.

This paper explores the possibility of using a whole atmosphere model combined with a data assimilation system to follow the real dynamics of the whole atmospheric system for the first time. The whole atmospheric data assimilation and forecast system is briefly described in the next section, followed by sections on the assimilation and forecast results on the January-February 2009 sudden stratospheric warming (SSW) and summary and conclusions.

**Corresponding author address:* Houjun Wang, CIRES, University of Colorado, Boulder, Colorado; e-mail: houjun.wang@colorado.edu.

2. THE WHOLE ATMOSPHRER DATA ASSIMILATION AND FORECAST SYSTEM

The whole atmosphere data assimilation and forecast system used in this study consists of a 3-dimensional variational (3D-Var) analysis system and a whole atmospheric model. The 3D-Var analysis system is the Gridpoint Statistical Interpolation (GSI) system of the National Centers for Environmental Prediction (NCEP), extended to be compatible with the whole atmospheric model. The whole atmospheric model is also an extension of the NCEP's Global Forecast System (GFS) model.

GSI is a unified analysis system for both regional and global data assimilations. The usual 3-dimensional variational (3D-Var) analysis technique is used in GSI (Wu, et al., 2002). It is used in the NCEP's operational data assimilation (DA) systems and in other research and quasi-real-time settings, such as with the WRF (Weather Research and Forecasting) model. NOAA Global System Division (GSD) is using the GSI as their next generation high frequency and high-resolution data assimilation and forecast system, or Rapid Refresh (RR). NASA GMAO uses GSI as a part of the NASA 4-Dimessional Variational (4D-VAR) data assimilation system. GSI is also becoming a community data assimilation system through the work in the Development Testbed Center (DTC), which provides a version of GSI that can be used easily on multiple platforms, and provides GSI documents and user supports for community researchers.

The forecast model used with GSI is the Whole Atmosphere Model (WAM), an extension of the NCEP's GFS model. The current GFS model has 64 model levels, with a top of model of about 60 km. WAM has 150 model levels, with a top of the model of about 600 km. It covers the regions of important ionospheric processes and their variability. WAM contains basic ionospheric effects on neutral atmosphere, i.e., ion drag and Joule heating. More sophisticated or realistic ionosphere-plasmasphere module is being developed and applied in WAM.

2.1 Modifications to GSI Analysis System

To use GSI with WAM, the background error (BE) statistics needed to be redefined. The BE statistics (i.e., forecast-error covariance) used in WAM-GSI was derived from the 24-hour difference/tendency in the 1-year WAM “free” runs (i.e., continuous runs without observational data injection/update). This is similar in spirit to the so-called NMC-method (NMC stands for National Meteorological Center, i.e., current NCEP) (Parish and Derber, 1992), but usually the BE statistics are derived from difference in a sample of short-term forecast of different lengths, e.g., 12 hour and 36 hour forecasts, valid at the same time (e.g., Belo Pereira and Berre, 2006). Considering the existence of the large diurnal variability in the upper atmosphere, the 24-hour difference in the forecast is used here. In the lower atmosphere, the derived standard deviations are somewhat overestimated: by about a factor of 3 compared to that used in the operational GFS-GSI system. Although the analysis appeared not to be significantly affected by these statistics, they were scaled down to the similar magnitude to match the operational statistics.

In addition, the Community Radiative Transfer Model (CRTM) is used in GSI for radiance assimilation. The pressure of the top of atmosphere/model is set to 0.005 hPa (corresponding to about 80 km) in CRTM. Although the pressure at the top of the WAM model of WAM is $1.5x10^{-9}$ hPa (about 600 km), the calculation of CRTM in WAM-GSI is restricted up to 0.005 hPa. The WAM-GSI analysis results appeared not affected by this restriction, since in this study, the WAM-GSI system only assimilates observational data used in the operational DA system up to about 0.1 hPa (about 60 km).

Finally, WAM has more trace gas components, i.e., it treats O, O_2, and N_2 separately, in addition to H_2O and O_3. Thus the input and output in GSI need to be modified correspondingly to handle the additional trace gas components.

2.2 Incremental Analysis Update (IAU)

Numerical experiments with WAM-GSI data assimilation system show that a typical convergence of GSI was obtained in the WAM-GSI system: GSI converges in less than 50 iterations. However, the conventional intermittent, 6-hourly cycling data assimilation strategy used in the WAM-GSI system produced excessive damping in the upper atmosphere. Important tides that were well simulated in long-term WAM “free” runs (Akmaev et al., 2008; Fuller-Rowell et al., 2010) were all severely damped by the digital filter required in the WAM-GSI data assimilation cycle. This pathological effect could not be remedied simply by tuning the digital filter used in the model. One way to remedy this damping of waves in the upper atmosphere was to update analysis incrementally into the model, thus avoid the need for the initialization procedure (e.g., digital filter in this case) during the forecast stage. We implemented the so-called Incremental Analysis Update (IAU) scheme (Bloom et al., 1996) into the WAM-GSI data assimilation cycle. Essentially in using the IAU scheme in WAM-GSI, (a) the analysis increments, i.e., the GSI analysis minus the first-guess (WAM forecasts), are created on the WAM physics grid after the GSI analysis; (b) then WAM is restarted from 3 hour earlier before the analysis time, and the increments are applied at each time step as a constant forcing spread over a 6-hour window center around the analysis time. The WAM-GSI-IAU system, or briefly WDAS (Whole atmosphere Data Assimilation System), significantly improved representation of tides waves in the upper atmosphere, as is shown in the results in the following section.

3. DATA ASSIMILATION AND FORECAST EXPERIMENTS FOR THE 2009 SSW

The whole atmosphere data assimilation and forecast system described above is used to simulate the January 2009 sudden stratospheric warming (SSW) event. The January 2009 SSW was a vortex split type of SSW. It was a significant event with a singular rapid polar cap temperature increase and especially the observed thermospheric and ionospheric responses. All conventional and satellite observational data used in the GDAS (NCEP’s operational Global DA System) are injected into the WDAS system. Typical convergence rate in GSI minimization iterations is normally achieved during WDAS DA cycle. In this section, we will show the polarcap temperature in the stratosphere at 10 hPa (~30 km altitude) from analysis and forecast. Space-time spectral analysis is also performed to show the major tidal wave responses in the E-region (dynamo region, 90-160 km altitudes) to the SSW.

3.1 Polar cap Temperature Changes at 10 hPa

The mean polar cap stratospheric temperature changes are well captured by the WDAS system. Figure 1 shows the two-month (1 January to 28 February 2009) time series of the 60° north polar cap temperature from the WDAS (red dash line) and the NCEP's operational Global Data Assimilation System (GDAS) (blue solid line). In both DA systems the average polar-cap temperature at 10 hPa (around 30 km altitude) increased more than 50 degree sharply within about 5 to 7 days, with a peak on 23 January 2009. Note that in the stratosphere, the WDAS analysis closely followed the one from the NCEP operational GDAS system.

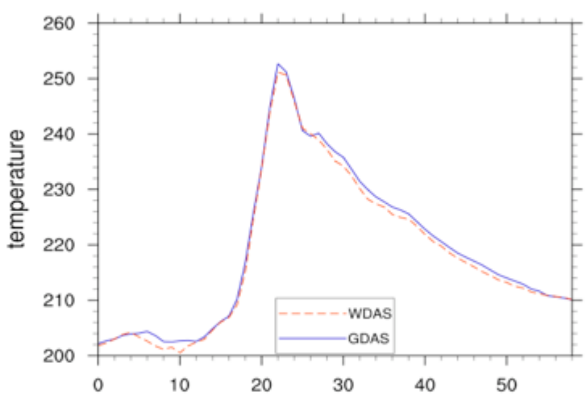

Fig. 1. Two-month time series of the mean 60N-polarcap temperature of the WDAS and GDAS analyses at 10 hPa from 1 Jan 2009 to 28 Feb 2009.

In addition, forecast experiments made from the analysis also show quite similar response of the polar-cap temperature changes many days in advance. Figure 2 shows the mean polar-cap temperature at 10 hPa from the extended (21-day) WAM forecast (WAM-FCST), initialized at 00 UTC on 15 January 2009 from WDAS analysis. For comparison, Figure 2 also shows results from the operational GFS medium-range (16-day) forecast (GFS-FCST), initialized at 00 UTC on 15 January 2009 from the GFS-GSI analysis and results from the WDAS analysis (WDAS-ANAL).

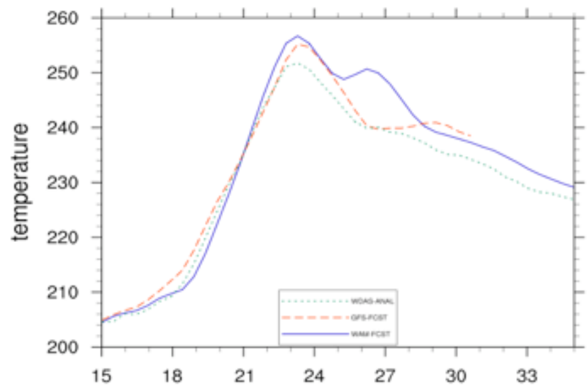

Fig. 2. Time series of the mean 60N-polarcap temperature at 10 hPa from WAM forecast (WAM-FCST: blue solid line) and GFS forecast (GFS-FCST: red dash line), initialized at 00 UTC 15 Jan 2009; compared with WDAS analysis (WDAS-ANAL: green dotted line).

3.2 Tidal Wave Responses in the E-Region

The standard space-time spectral analysis (e.g., Wheeler and Kiladis, 1999) was applied to the hourly model output of the WDAS data assimilation and forecast system. The data were grouped in 3-days and linear trends were removed. We are specifically interested in the changes in tidal waves during the 2009 SSW event.

The migrating SW2 (semidiurnal, westward propagating, zonal wave number 2) waves are major E-region dynamo wind contributor. The migrating TW3 (terdiurnal, westward propagating, zonal wave number 3) waves were also found under significant changes in a WAM model-generated moderate SSW (Fuller-Rowell et al., 2010). Figure 3 shows the maximum SW2 and TW3 wave amplitudes of the zonal wind from WDAS analysis. The maxima are located in the E-region (see also Figures 5 and 6) and are shown for the northern hemisphere (NH) and southern hemisphere (SH) separately. Several features of E-region tidal wave responses to the 2009 SSW event can be identified from Figure 3:

(a) SW2 attained its maxima in NH about 10 days after the SSW peak temperature, quite closely followed the stratospheric warming trend earlier, indicating strong influence from lower atmospheric planetary waves (PWs). In response to SSW, the peak SW2 amplitudes increased about 45 ms^{-1} in about 10 days, reaching 75 ms^{-1};

(b) TW3 started to increase when SSW began and while SW2 was declining (see also Figures 5 and 6). The peak TW3 amplitudes increased about

20 ms^{-1} in about 3 days from its background value of about 10 ms^{-1}. It is highly possible that resonant nonlinear wave-wave interactions (between SW2, DW1=diurnal, westward propagating, zonal wave number 1, and TW3) have contributed to the rapid growth of TW3 in the early stage of SSW (notice that DW1 waves are at relative low amplitudes compared to SW2 and TW3 waves at these altitudes); and

(c) Global responses to SSW are indicated in the changes of these waves in the SH.

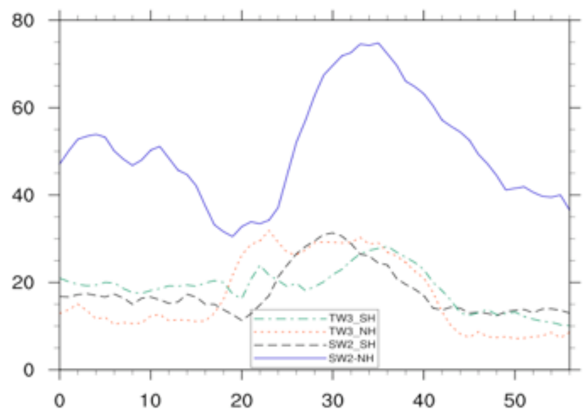

Fig. 3. Time series of the maximum amplitudes of SW2 and TW3 waves in the WDAS analysis from 2 Jan 2009 to 27 Feb 2009. The maxima are shown for the northern hemisphere (NH) and southern hemisphere (SH) separately.

Figure 4 shows the maxima of SW2 and TW3 wave amplitudes of the zonal wind, as Figure 3, but for the extended (21-day) WAM forecasts in comparison with the WDAS analysis. Only northern hemisphere (NH) maxima are shown. It shows that the WAM forecasts initialized from WDAS analysis are remarkably consistent with the WDAS analysis, indicating a great forecasting capability of the WDAS system, several days, even weeks in advance.

Figure 5 is the latitudinal-vertical view of the SW2 and TW3 amplitudes of the zonal wind from the WDAS analysis during the 2009 SSW. Model levels from 80-130 (~70-230 km) are shown in the vertical. Large SW2 waves are found in the middle latitude (e.g., from 30N to 70N) and from model level 100 to 115 (about 100 to 140 km), important for the E-region dynamo effects. The maxima of the TW3 wave amplitude maxima are found to be higher than that of the SW2 waves, with TW3 maxima around model level 120 (around 160 km, in the upper E-region and lower F-region) and SW2 maxima around model level 110 (around 110 km Very similar results to Figure 5 for are obtained from the extended (21-day) WAM forecasts, initialized from the WDAS analysis at 00 UTC on 15 Jan 2009 (not shown, but see Figure 4).

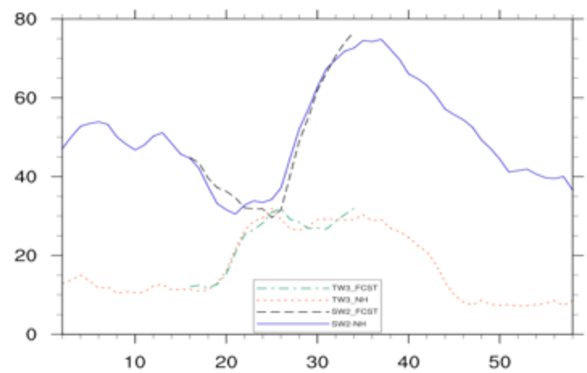

Fig. 4. Time series of the maximum amplitudes of SW2 and TW3 waves: comparing the WAM forecast with the WDAS analysis from 2 Jan 2009 to 27 Feb 2009. The 21-day forecast (FCST) was initialized at 00 UTC 15 Jan 2009. Only the maxima in the northern hemisphere (NH) are shown.

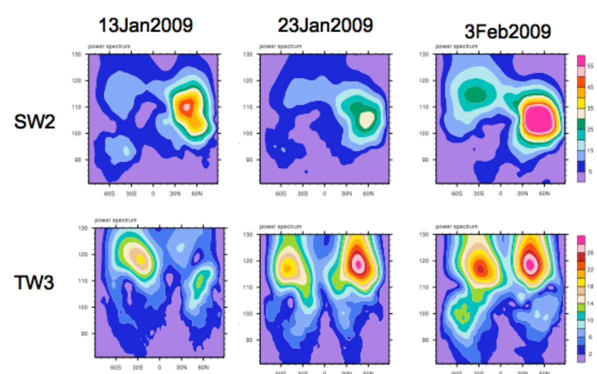

Fig. 5. The latitudinal-vertical view for the SW2 and TW3 wave amplitudes of the zonal wind from the WDAS analysis, showing their changes before (13 Jan 2009, left panels), on (23 Jan 2009, middle panels), and after SSW (3 Feb 2009, right panels). Note the different color scales: the SW2 waves are drawn from 5 to 55 ms^{-1} with an interval of 5 ms^{-1} and the TW3 waves are drawn from 2 to 28 ms^{-1} with an interval of 2 ms^{-1}.

To better illustrate the possible wave-wave interactions between SW2 and TW3 waves, Figure 6 shows the SW2 and TW3 wave amplitudes of zonal wind on Jan 13 and 23, 2009 (same dates as the left and middle panels in Figure 5) and on

Jan 21, 2009, drawn on the same color scale as that of TW3 waves in Figure 5. This quite clearly indicates the "conversion" of SW2 waves (in interacting with DW1 waves) to TW3 waves in the upper E-region.

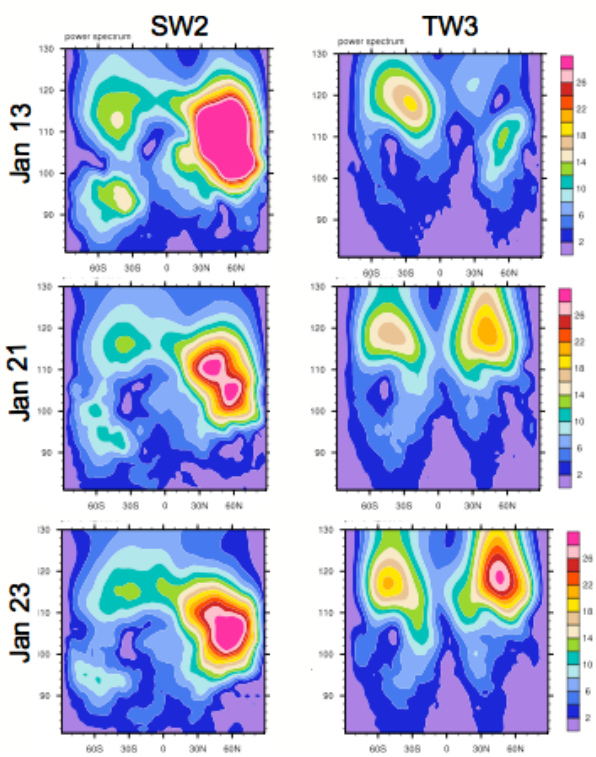

Fig. 6. The latitudinal-vertical view for the SW2 and TW3 wave amplitudes of the zonal wind from the WDAS analysis on Jan 13, 21 and 23, 2009, drawn on the same color scale from 2 to 28 ms^{-1} with an interval of 2 ms^{-1}.

4. SUMMARY AND CONCLUSIONS

In this work we explore whole atmosphere data assimilation and forecast with a whole atmosphere model and a 3D-Var analysis system for the first time. The NCEP's GSI 3D-Var analysis system is extended to work with the whole atmosphere model (WAM), and an incremental analysis update (IAU) scheme is implemented in the data assimilation cycle. The IAU scheme effectively removed the problem of excessive damping, by digital filter, of important waves in the upper atmosphere. These upward propagating waves significantly influence ionosphere, thus it is vital to have representative signatures of these waves in the analysis fields for successful simulation of ionospheric variability.

The whole atmosphere data assimilation system (WDAS) thus formed is used to conduct data assimilation and forecast experiments for the 2009 sudden stratospheric warming (SSW) events. We found that:

(a) Good agreement is found between WDAS analysis and the NCEP's operational GDAS analysis in the stratosphere (presumably in the other part of lower atmosphere where the WDAS and GDAS analyses overlap);

(b) Tidal wave analysis shows significant increase in both SW2 and TW3 wave amplitudes in the E-region. These enhancements could have significant impact on the E-region dynamo, hence ionospheric electrodynamics;

(c) The increase of SW2 during SSW is attributed to influence of upward propagation of planetary waves from the lower atmosphere, while the rapid growth of TW3 in the early stage of SSW is attributed largely to the resonant wave-wave interactions between SW2, DW1 and TW3;

(d) These tidal wave responses during SSW appeared to be global in scale; and

(e) The extended forecasts showed fairly consistent tidal wave responses to the SSW event, indicating a potential forecasting capability of several days even week in advance of the effect of the large-scale tropospheric and stratospheric dynamics on ionosphere and thermosphere.

Currently, the WDAS system uses only observational data that are used in the current GDAS operational data assimilation system. We are exploring the potential of injecting other upper atmosphere observational data, such as SABER or MLS data, updating the model background error statistics, and high-frequency data assimilation.

5. ACKNOWLEDGEMENTS

Discussions with many of our colleagues have been very helpful at the different stages of this research. We would like to acknowledge in particular the valuable help we received from Dr. M. Hu on using GSI with WAM, D. Kleist for preparing the background error statistics, and R. Treaton for answering various GSI-related questions. The funding for this research is provided by the NASA's Heliophysics Theory Program and the AFOSR's MURI NADIR grant.

6. REFERENCES

Akmaev, R. A., T. J. Fuller-Rowell, F. Wu, J. M. Forbes, X. Zhang, A. F. Anghel, M. D. Iredell, S. Moorthi, and H.-M. Juang (2008), Tidal variability in the lower thermosphere: Comparison of Whole Atmosphere Model (WAM) simulations with observations from TIMED, *Geophys. Res. Lett.*, 35, L03810, doi:10.1029/2007GL032584.

Belo Pereira, M. and L. Berre, 2006: The use of an Ensemble approach to study the Background Error Covariances in a Global NWP Model. Mon.Wea.Rev., 134, 2466-2489.

Bloom, S. C., L. L. Takacs, A. M. da Silva, and D. Ledvina, 1996: Data assimilation using Incremental Analysis Updates. *Mon. Wea. Rev.*, **124**:1256–1271.

Chau, J. L., N. A. Aponte, E. Cabassa, M. P. Sulzer, L. P. Goncharenko, and S. A. González (2010), Quiet time ionospheric variability over Arecibo during sudden stratospheric warming events, *J. Geophys. Res.*, 115, A00G06, doi:10.1029/2010JA015378.

Fuller-Rowell, T., F. Wu, R. Akmaev, T.-W. Fang, and E. Araujo-Pradere (2010), A whole atmosphere model simulation of the impact of a sudden stratospheric warming on thermosphere dynamics and electrodynamics, *J. Geophys. Res.*, 115, A00G08, doi:10.1029/2010JA015524.

Kalnay, E., 2002: Atmospheric Modeling, Data Assimilation and Predictability, Cambridge University Press, 364 pp.

Parrish, D. F., and J. Derber, 1992: The National Meteorological Center's spectral statistical interpolation analysis system. *Mon. Wea. Rev.,***120,** 1747–1763.

Wheeler, M., and G.N. Kiladis, 1999: Convectively coupled equatorial waves: Analysis of clouds and temperature in the wavenumber-frequency domain. *J. Atmos. Sci.*, 56, 374-399.

Wu, W. S., R. J. Purser, D. F. Parrish, 2002: Three-dimensional variational analysis with spatially inhomogeneous covariances. *Mon. Wea. Rev.*, **130**, 2905–2916.